Journal of Solid State Chemistry **151,** 267–271 (2000)
doi:10.1006/jssc.2000.8650, available online at http://www.idealibrary.com on IDEAL®

Sr(OH)Br, a Metal Hydroxide Halide with Unusual Properties

S. Peter,* F. Altorfer,† W. Bührer,†,‡,[1] and H. D. Lutz*

*Anorganische Chemie I, Universität Siegen, D-57068 Siegen, Germany; †Laboratory for Neutron Scattering, Paul Scherrer Institute & ETH Zurich Villigen, CH-5232 Villigen-PSI, Switzerland; ‡University of Maryland, College Park, Maryland 20742; and National Institute of Standards and Technology, Gaithersburg, Maryland 20899 USA

Received November 23, 1999; in revised form February 1, 2000; accepted February 10, 2000

The disorder of the hydroxide ions of the cubic polymorph of strontium hydroxide bromide Sr(OH)Br(*cP*16) between the two OH^- ion positions I and II has been studied by differential scanning calorimetry (DSC), impedance spectroscopy (electric conductivity), and temperature-dependent Raman spectroscopy (90–630 K). We found that the OH^- position I, which is involved in weak trifurcated O–H ⋯ Br hydrogen bonds (ν_{OH} = 3543 cm^{-1} at 298 K), is depopulated with increasing temperature in favour of OH^- position II, where the OH^- ions form stronger linear hydrogen bonds (ν_{OH} = 3492 cm^{-1}). The O ⋯ Br distance of the latter bond decreases from 10 to 780 K by about 5 pm and, hence, the strength of the respective hydrogen bond increases. This is obviously the reason for the change of the population ratio OH^- (II)/OH^- (I) with increasing temperature, as revealed from both neutron diffraction and Raman spectroscopic data, e.g., 0.08 at 10 K and 0.34 at 780 K (neutron data). For the deuterated compound, these ratios are smaller because in the case of linear hydrogen bonds (OH^- II) the strength of D bonds is somewhat greater than that of H bonds and vice versa in the case of trifurcated bonds (OH^- I). This is caused by the different zero-point vibrational amplitudes of the respective librational modes. At elevated temperatures, Sr(OH)Br displays large protonic conductivity σ with an activation energy of conduction of 60.5 kJ mol^{-1} (500–670 K), exceeding $\sigma > 10^{-2}\ \Omega^{-1}\ cm^{-1}$ above 700 K after a precipitous increase of σ by 2 orders of magnitude at about 673 K. As shown from the half-widths of the Raman bands the dynamics of local motions of the OH^- ions is at least 1 order of magnitude faster than the macroscopic diffusion processes.

Key Words: **strontium hydroxide bromide; Raman spectroscopy; differential scanning calorimetry; disorder of hydroxide ions; H/D isotopic effects; protonic conductivity.**

INTRODUCTION

The hitherto unknown compound Sr(OH)Br has been established to be dimorphic (1, 2). The monoclinic form Sr(O)Br(*mC*16), which is obtained on dehydration of $Sr(OH)Br \cdot 4H_2O$ (3), is metastable. It is converted into the stable cubic form Sr(OH)Br(*cP*16) on heating above 660 K. This polymorph crystallizes in the space group $P2_13$ with four formula units in the unit cell. The lattice constant *a* is 675.79(2) pm (1).

Cubic strontium hydroxide bromide displays disorder of the hydroxide ions from a position with weak trifurcated (four-center) OH ⋯ Br hydrogen bonds to stronger, nearly linear hydrogen bonds (see Fig. 1). The former position is preferred at low temperatures, the latter at elevated ones as shown from infrared spectroscopic measurements (1). Very recently, this has been confirmed by high-temperature neutron diffractometry (4). In order to examine the nature of and the reason for this behavior in more detail we studied the temperature dependence of the disorder and possible protonic conductivity by high-temperature Raman spectroscopy, impedance spectroscopy methods, and differential scanning calorimetry.

EXPERIMENTAL

Polycrystalline samples of Sr(OH)Br(*cP*16) were prepared by annealing stoichiometric amounts of anhydrous $Sr(OH)_2$ and $SrBr_2$ in carbon glass crucibles under argon at 845 K (1, 2, 5, 6). Sr(OH)Br(*mC*16) was obtained by dehydration of $Sr(OH)Br \cdot 4H_2O$ (3) at 520 K in a vacuum (10 Pa) (1, 2).

Differential scanning calorimetry (DSC) measurements were carried out on a Perkin Elmer DSC 7 system with samples of 10–20 mg. Gold crucibles were used as sample holders (cold welding). Heating rates were 20 K min^{-1}. Al_2O_3 was used as reference. Calibration of the apparatus was performed with the melting temperature and the heat of fusion of KNO_3.

Raman spectra, with the samples in closed glass capillaries, were measured on a Dilor OMARS multichannel Raman spectrograph (resolution $< 4\ cm^{-1}$) using the right-angle geometry. The 514.5 nm line of an argon ion laser was employed for excitation. Low-temperature Raman spectra

[1] Dr. Bührer died in November 1997.

0022-4596/00 $35.00

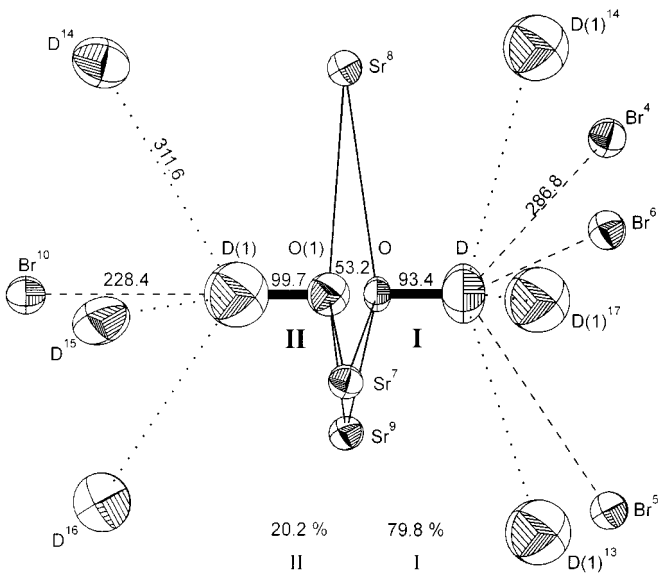

FIG. 1. Coordination of the OD^- ions of Sr(OD)Br(*cP*16) at 298 K (occupation factors of the positions I and II; distances, pm; - - -, hydrogen bonds) (1).

were recorded with the use of the variable-temperature cell Coderg model CRN2 (90–300 K). The Raman high-temperature measurements were performed using a specially designed high-temperature cell described in (5, 7) with the Eurotherm PID controller 818b and the Eurotherm thyristor controlling unit 425. The temperature uncertainty was < 3 K. For each spectrum, the cell was kept at constant temperature for 5–10 min.

The impedance diagrams (5 Hz–13 MHz) were determined with a Hewlett-Packard 4192A LF impedance analyzer. The heating rates were 1 K min^{-1}, the stepwidths 10 K h^{-1}. Details of the cell and the setup employed are given in (8).

RESULTS

1. *Differential Scanning Calorimetry (DSC) Measurements*

DSC thermograms of Sr(OH)Br(*cP*16) display two endothermic peaks at 685 and 722 K (see Fig. 3.3. in (2)) below that due to melting at 863 K (onset 848 K (5)). The transition energies are 1.1 and 2.7 kJ mol^{-1}, respectively (2, 4), and the energy of fusion is 22.4 kJ mol^{-1} (6).

2. *High-Temperature Raman Spectra*

High-temperature Raman spectra (in (9) called thermo-Raman spectra) of Sr(OH)Br in the OH stretching mode region are shown in Fig. 2. The spectra reveal both the monotropic phase transition of the monoclinic polymorph into the cubic one (2), and the temperature evolution of the frequencies, the half-widths, and the relative intensities of the two OH stretches of Sr(OH)Br(*cP*16). The two bands are due to the different arrangement of the disordered OH^- ions. Hence, their relative intensities display the respective occupation of the two positions as shown in Fig. 3. The red shift of the band at 3543 cm^{-1} with increase in temperature indicates bent or bifurcated hydrogen bonds, and the blue shift to the doublet at 3492 and 3478 cm^{-1} hints of linear or only weakly bent bonds (see the discussion given in Refs. (10, 11)). The increase of the half-width of the former band with increasing temperature is also shown in Fig. 3. In contrast, the half-width of the latter bands does not change very much in the temperature range between 110 and 673 K. This may be due to overlap of two bands (see Fig. 2).

3. *Electric Conductivity (Impedance Spectroscopy)*

The temperature evolution of the electric (protonic) conductivity of cubic Sr(OH)Br is shown in Fig. 4. As shown in

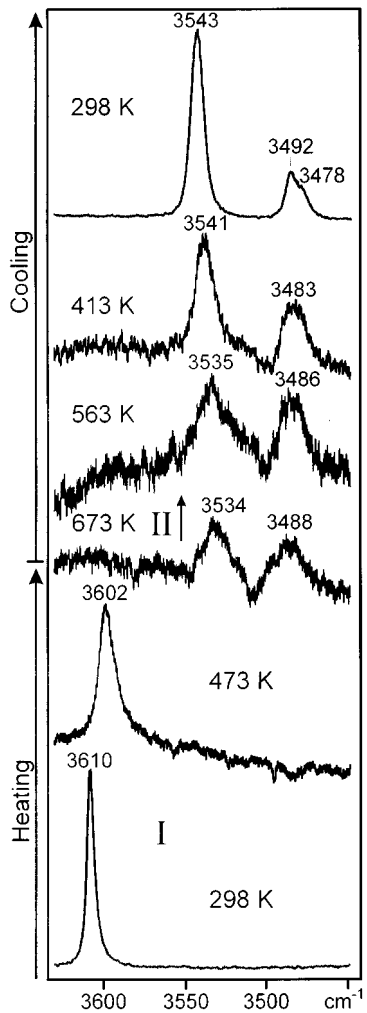

FIG. 2. High-temperature (Thermo) Raman spectra of Sr(OH)Br in the OH stretching mode region (I, Sr(OH)Br(*mC*16); II, Sr(OH)Br(*cP*16)).

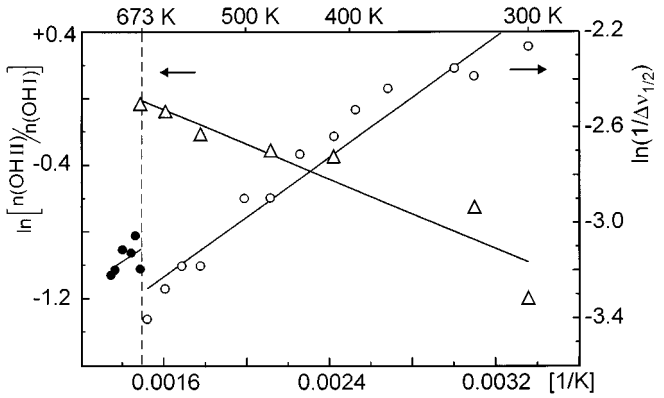

FIG. 3. Temperature dependence of both the occupation ratios of the two hydrogen positions (△) and the half-width (fwhm) of the OH stretching modes (○, ●) of Sr(OH)Br($cP16$) (ln(nOH I)/n(OH II)) vs $1/T$ and ln $\Delta\nu_{-}$ vs $1/T$; ○, below 673 K; ●, above the possible phase transition at 663 K; Raman spectroscopic data).

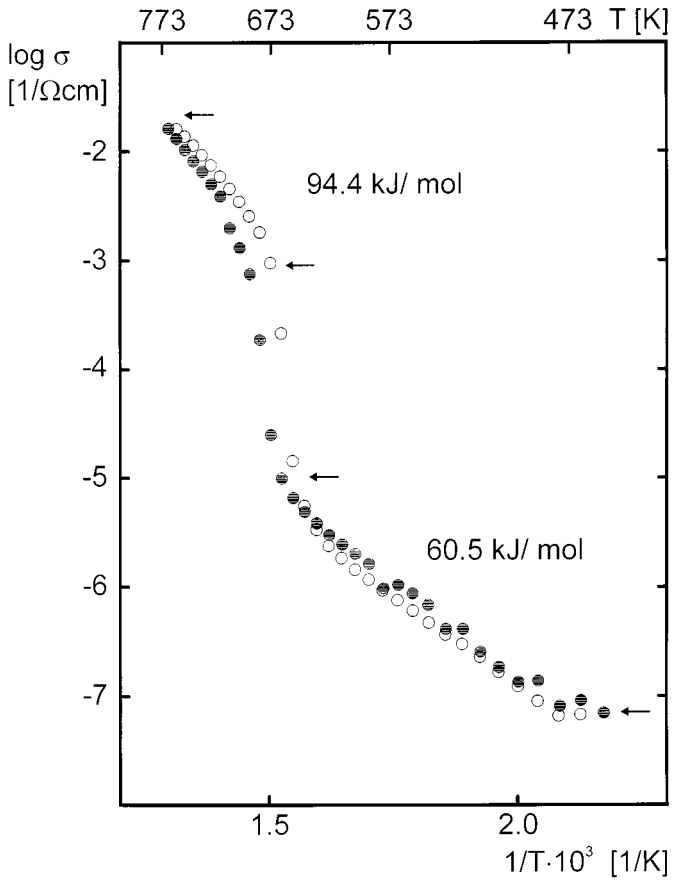

FIG. 4. Arrhenius plot of the electric (protonic) conductivity and activation energies of conduction of Sr(OH)Br($cP16$) (●, heating; ○, cooling).

the figure the conductivity data obtained display an Arrhenius-type ($\log\sigma$ vs $1/T$) behavior with an activation energy for conduction around 60.5 kJ mol^{-1} in the range up to 673 K. Between this temperature and about 700 K there is a precipitous increase in the conductivity by 2 orders of magnitude. Above 700 K to 773 K, again an Arrhenius-type behavior is observed but with greater activation energy (94.4 kJ mol^{-1}). The precipitous increase of the protonic conductivity of Sr(OH)Br($cP16$) just below 700 K has been observed in all the samples studied.

DISCUSSION

1. *Disorder of the Hydroxide Ions, Temperature Dependence*

As shown by both the high-temperature neutron scattering experiments (see Tables 1 and 2 and (4)) and the high-temperature Raman spectra the relative population of the two hydrogen positions of disordered Sr(OH)Br($cP16$) changes greatly with increasing temperature. Thus, at 10 K the position due to the stronger linear hydrogen bonds (OH^- II) is only populated by 8%; at 780 K, however, the

TABLE 1
Lattice Constants a, Fractional Atomic Coordinates $x\,(=y=z)$, and Occupation Factor n(H(II)) of Sr(OH)Br($cP16$) at Temperatures from 10 to 780 K (Space Group $P2_13$, $Z=4$) (4)

	10 K	150 K	300 K	480 K	590 K	670 K	780 K
a (pm)	672.79(1)	673.49(1)	674.88(2)	677.70(1)	678.89(2)	680.15(2)	681.71(2)
Sr	0.5710(3)	0.5727(3)	0.5714(5)	0.5727(6)	0.5720(6)	0.5728(3)	0.5718(5)
Br	0.8443(3)	0.8448(3)	0.8453(5)	0.8464(3)	0.8488(7)	0.8484(4)	0.8481(6)
O	0.1721(5)	0.1738(7)	0.1701(11)	0.1722(8)	0.1712(16)	0.1692(9)	0.1694(12)
H	0.2531(10)	0.2530(11)	0.2549(18)	0.2469(16)	0.2479(35)	0.2435(17)	0.2448(24)
O(1)	0.1250(5)	0.1237(57)	0.1267(60)	0.1205(20)	0.1201(43)	0.1228(25)	0.1284(35)
H(1)	0.028(9)	0.042(12)	0.046(6)	0.0456(33)	0.0456(84)	0.0356(43)	0.0342(24)
n(H(1))	0.076(10)	0.104(12)	0.162(14)	0.242(11)	0.230(26)	0.240(13)	0.252(19)

TABLE 2
Selected Interactomic Distances (pm) of Sr(OH)Br(*cP*16) at Temperatures from 10 to 780 K

	10 K	150 K	300 K	480 K	590 K	670 K	733 K
				OH^- I			
O–H	94.4(8)	92.4(8)	99.1(14)	87.7(12)	90.2(26)	87.5(13)	89.0(18)
O ⋯ Br	345.5(4)	344.3(4)	347.9(8)	347.2(6)	347.7(12)	350.2(7)	351.0(9)
H ⋯ Br	285.3(7)	285.5(8)	284.8(13)	290.7(11)	289.8(24)	293.3(12)	293.2(17)
				OH^- II			
O(1)–H(1)	106.6(39)	87.4(53)	94.1(56)	87.9(26)	87.6(64)	102.7(34)	108.9(44)
O(1) ⋯ Br	327.1(4)	325.3(36)	328.9(41)	321.7(14)	319.0(30)	323.3(17)	328.6(24)
H(1) ⋯ Br	220.5(29)	238.0(40)	234.8(39)	233.8(22)	231.4(57)	220.5(29)	219.7(38)
O–O(1)	54.9(5)	58.4(36)	50.7(41)	60.7(15)	60.1(31)	54.7(18)	50.8(26)

population is 25% (neutron powder data (4)). The change in the relative population of the two sites obeys a Boltzmann-type behavior.

From the slope of the obtained straight lines (see Fig. 3), i.e., $\ln(n_{OH(I)}/n_{OH(II)})$ vs $1/T$, 4.32 kJ mol^{-1} (Raman data) and 1.73 kJ mol^{-1} (neutron data (4)) have been derived as energy parameters in the ranges 300–733 K and 10–780 K, respectively. For an interpretation of these energies, however, which are in the order of bond energies of weak hydrogen bonds, for example, with respect to the energy difference of the two OH^- ion positions, caution should be exercised. Thus, the obtained values resemble those derived from the temperature evolution of the half-widths of the Raman band due to OH^- (I), viz. 5.21 and 4.74 kJ mol^{-1} (see Table 3). These energies, which correspond to 436 and 396 cm^{-1}, are obviously not due to vibrational dephasing processes (12, 13) because the OH librations and lattice vibrations of Sr(OH)Br(*cP*16) are observed at 660 cm^{-1} and below 350 cm^{-1}.

2. *Strength of the Hydrogen Bond, H/D Isotopic Effects*

The O ⋯ Br and H ⋯ Br distances of the two hydrogen bonds present in Sr(OH)Br(*cP*16) change in a different manner with increasing temperature (see Tables 1 and 2 and Fig. 5). Thus, the four-center (trifurcated) bond due to OH^- (I) elongates somewhat with the increase in temperature as usual with the thermal expansion of matter. The linear bond of OH^- (II), however, shortens on going from 10 to 780 K (see Table 2 and Fig. 5). This means that the latter bond is strengthened at high temperatures, which is also revealed from the lack of positive temperature shift of the respective OH stretching mode (see Fig. 2) expected for linear hydrogen bonds (11). (The relatively large negative temperature shift of the OH stretch due to OH^- (I) ($dv_{OH}/dT < 0$) is caused by the trifurcated nature of that bond (11).) The increase in hydrogen bond strength of OH^- (II) with increasing temperature is obviously the reason for the increased population of that OH^- position at high temperatures.

The relative population of the two OH^- ion positions differs significantly on going from the protonated compound to the deuterated one. This is revealed by the relative intensities of the respective OH and OD stretches as well as by the results of the neutron diffraction data. Thus, the ratio of the occupation factors of OH^- (II)/OH^- (I) is 0.182 at ambient temperature, and that of OD^- (II)/OD^- (I) is 0.253 (1, 2). The respective Raman data are 0.201 and 0.299.

TABLE 3
Energies of the Boltzmann Distribution between the Two OH^- Ion Positions (E_b) and Activation Energies Due to the Increase of the Half-Widths of the OH Stretches (V_a) (see Fig. 3)

	Temp, K	E_b or V_a, kJ mol^{-1}	E_b or V_a, cm^{-1}	E_b or V_a, K	C^a	r^b
Raman	110–300	0.95	79	114	− 0.82	1
	300–673	4.32	361	520	0.77	0.89
$\Delta v(OH^-$ I)	110–300	0.49	41	58	− 2.46	1
	300–658	5.21	436	627	− 4.23	0.94
	673–743	4.74	396	570	− 3.96	0.26

[a] Prefactor of Boltzmann's and Arrhenius's equations, respectively.
[b] Straight-line correlation coefficient.

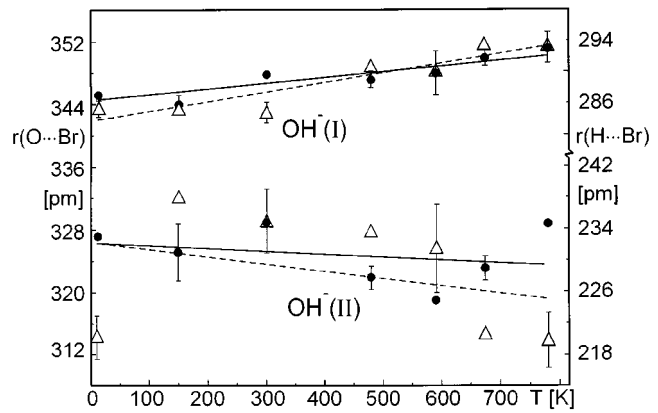

FIG. 5. Temperature dependence of the hydrogen-bond distances O ··· Br (●) and H ··· Br (△) due to the hydrogen positions I and II of Sr(OH)Br(*cP*16) (—— and - - -, linear fits of the data).

Hence, the strength of H hydrogen bonds at site I exceeds that at site II to a larger extent than in the case of D hydrogen bonds. This means that the difference in the strengths of the respective hydrogen bonds is mainly governed by the different zero-point vibrational amplitudes of the librational modes as usually found in the case of weak hydrogen bonds of solid hydroxides (11, 14). Thus, in the case of linear hydrogen bonds as at position II, D ··· Br hydrogen bonds are stronger than H ··· Br bonds, and in the case of trifurcated bonds as at position I, H ··· Br bonds are stronger than D ··· Br bonds (see Fig. 6).

3. Dynamics of the Hydroxide Ions, Protonic Conductivity

The strong increase of all the half-widths of the respective Raman bands (see Figs. 2 and 3), the displacement parameters of the hydrogen atoms (4), and the electric conductivity (impedance spectroscopy, see Fig. 4) demonstrate increasing dynamic processes for the title compound at high temperatures. Obviously, there are increasing librational motions of the OH^- ions, more frequent changes of the their lattice sites, i.e., changes between the positions I and II, and at temperatures above 673 K increased protonic conductivity. The latter are shown by the endothermic peaks at 685 and 722 K in the DSC diagrams, the precipitous change of the half-width of the Raman band due to OH^- (I) (see Fig. 3), and particularly the likewise precipitous increase in the electric conductivity at that temperature (see Fig. 4).

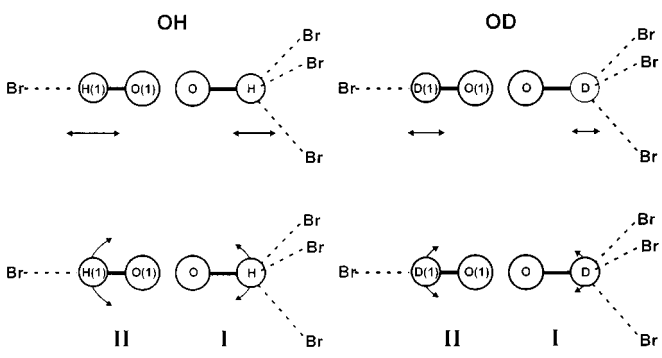

FIG. 6. Schematic picture of the zero-point vibrational amplitudes of the OH(D) stretching vibrations and librations of Sr(OH)Br(*cP*16) and Sr(OD)Br(*cP*16).

The nature of the mechanism of the observed protonic conductivity of the title compound, for example, a Grotthus mechanism a low temperature and a vehicle mechanism at higher ones, as found for other hydroxides and basic oxides (15), is not fully known so far (2) (and speculations on it should be avoided). Thus, it cannot be fully excluded if impurities or partial decomposition processes are the reason for the very high electric conductivity of Sr(OH)Br(*cP*16) as has been established very recently for the high-temperature conductivity of alkali metal hydroxides (16). It is true that the dynamics of the local motions is at least 1 order of magnitude faster than the diffusion processes due to the macroscopic electric conductivity.

ACKNOWLEDGMENTS

The authors gratefully acknowledge financial support by the Bundesminister für Bildung, Wissenschaft, Forschung und Technologie under contract 332-4003-03-LU4SIE 7, the Deutsche Forschungsgemeinschaft under contract Lu 140/32-1, and the Fonds der Chemischen Industrie.

REFERENCES

1. S. Peter and H. D. Lutz, *Z. Anorg. Allg. Chem.* **624,** 1067 (1998).
2. S. Peter, Ph. D. Thesis, University of Siegen, 1997.
3. Th. Kellersohn, K. Beckenkamp, and H. D. Lutz, *Z. Naturforsch. B* **96,** 1279 (1991).
4. F. Altorfer, H. D. Lutz, and S. Peter, *Physica B* **280,** 276 (2000).
5. K. Beckenkamp, Ph. D. Thesis, University of Siegen, 1991.
6. K. Beckenkamp and H. D. Lutz, *Thermochim. Acta* **258,** 189 (1995).
7. H. D. Lutz, K. Beckenkamp, and S. Peter, *Spectrochim. Acta A* **51,** 755 (1995).
8. H. D. Lutz, A. Pfitzner, and Ch. Wickel, *Solid State Ionics* **48,** 131 (1991).
9. H. Chang and P. J. Huang, *Anal. Chem.* **69,** 1485 (1997).
10. H. D. Lutz, K. Beckenkamp, and H. Möller, *J. Mol. Struct.* **322,** 263 (1994).
11. H. D. Lutz, *Struct. Bonding* (*Berlin*) **82,** 85 (1995).
12. T. E. Jenkins and J. Lewis, *J. Raman Spectrosc.* **11,** 1 (1981).
13. H. D. Lutz, J. Henning, H. Jacobs, and B. Harbrecht, *Ber. Bunsenges. Phys. Chem.* **92,** 1557 (1988).
14. H.D. Lutz, K. Beckenkamp, and H. Möller, *J. Mol. Struct.* **322,** 263 (1994).
15. K.-D. Kreuer, *Chem. Mater.* **8,** 610 (1996).
16. M. Spaeth, K. D. Kreuer, Th. Dippel, and J. Maier, *Solid State Ionics* **97,** 291 (1997).